Article

Clinical Validation of a New Enhanced Stent Imaging Method

Chadi Ghafari [1], Khalil Houissa [2], Jo Dens [3], Claudiu Ungureanu [1,4], Peter Kayaert [5], Cyril Constant [6] and Stéphane Carlier [1,7,*]

[1] Department of Cardiology, University of Mons (UMONS), 7000 Mons, Belgium; chadi.ghafari@umons.ac.be (C.G.); claudiu-mih.ungureanu@jolimont.be (C.U.)
[2] Department of Cardiology, Military Hospital of Tunis, Tunis 1000, Tunisia; khalilhouissa@gmail.com
[3] Cardiology Department, Ziekenhuis Oost-Limburg, 3600 Genk, Belgium; jo.dens@zol.be
[4] Cardiology Department, Hopital Jolimont, 7100 La Louvière, Belgium
[5] Cardiology Department, Jessa Ziekenhuis, 3500 Hasselt, Belgium; peter.kayaert@jessazh.be
[6] Faculty of Medicine, Free University of Brussels (ULB), 1050 Bruxelles, Belgium; cyril.constant@ulb.ac.be
[7] Cardiology Department, CHU Ambroise Paré, 7000 Mons, Belgium
* Correspondence: stephane.carlier@umons.ac.be

Abstract: (1) Background: Stent underexpansion is the main cause of stent thrombosis and restenosis. Coronary angiography has limitations in the assessment of stent expansion. Enhanced stent imaging (ESI) methods allow a detailed visualization of stent deployment. We qualitatively compare image results from two ESI system vendors (StentBoost™ (SB) and CAAS StentEnhancer™ (SE)) and report quantitative results of deployed stents diameters by quantitative coronary angiography (QCA) and by SE. (2) Methods: The ESI systems from SB and SE were compared and graded by two blinded observers for different characteristics: 1 visualization of the proximal and distal edges of the stents; 2 visualization of the stent struts; 3 presence of underexpansion and 4 calcifications. Stent diameters were quantitatively measured using dedicated QCA and SE software and compared to chart diameters according to the pressure of implantation. (3) Results: A total of 249 ESI sequences were qualitatively compared. Inter-observer variability was noted for strut visibility and total scores. Inter-observer agreement was found for the assessment of proximal stent edge and stent underexpansion. The predicted chart diameters were 0.31 ± 0.30 mm larger than SE diameters ($p < 0.05$). Stent diameters by SE after post-dilatation were 0.47 ± 0.31 mm smaller than the post-dilation balloon diameter ($p < 0.05$). SE-derived diameters significantly differed from QCA; by Bland–Altman analysis the bias was -0.37 ± 0.42 mm ($p < 0.001$). (4) Conclusions: SE provides an enhanced visualization and allows precise quantitative assessment of stent expansion without the limitations of QCA when overlapping coronary side branches are present.

Keywords: stent; percutaneous coronary intervention; quantitative coronary angiography

1. Introduction

Coronary angiography is the primary diagnostic imaging modality for the evaluation and classification of coronary artery lesions as well as for guiding percutaneous coronary interventions (PCIs). Percutaneous interventions are the most performed coronary revascularization procedure, improving the quality of life of patients along with their clinical outcomes [1]. Despite major advances in coronary stent technology, acute and late PCI-related complications still occur [2–4]. Successful PCI results relate directly to proper stent placement and deployment. Stent underexpansion was shown to be a major predictor of stent restenosis and thrombosis by quantitative coronary angiography (QCA) [5]. Moreover, insufficient stent expansion and malapposition found by intracoronary imaging were shown as major predictors of stent thrombosis in several studies [6–10].

Although optimizing stent implantation under intravascular imaging guidance is widely supported by the current literature [11–17], its routine clinical use remains limited

due to the added time and cost to the procedure along with the image interpretation difficulties. Despite conventional angiography often falling behind in the detection of stent underexpansion and presenting a suboptimal accuracy assessing stent position, it is still carried out during routine clinical practice especially with newer generation scaffolds that are implanted at a higher pressure followed by a post-dilatation step and rely on the radiopaque nature of the material used for visualization.

Thicker stent struts were associated with higher in-stent restenosis rates in the ISAR STEREO trials [18,19]. On the other hand, thinner strut scaffolds used in new generation stents have been advocated to significantly reduce the risk of myocardial infarction at the expense of being more radiolucent on fluoroscopy [3,20–23]. Moreover, the trend towards the use of lower X-ray power during angiographic procedures presents another challenge for stent visualization which is further altered due to motion during the angiography sequence secondary to X-ray scattering.

More recently, several enhanced stent imaging (ESI) methods have been developed. These angiography-based software improve stent visualization and provide quantitative as well as qualitative data post-stent deployment but remain dependent on the X-ray angiographic system of each vendor [24,25]. The StentBoost® system (SB) (Philips Healthcare, Andover, MA, USA) is a motion-corrected X-ray stent visualization software that allows better assessment of stent expansion without using contrast [25]. It was designed as an add-on to conventional X-ray angiographic system and was found to be superior to conventional angiography in detecting stent underexpansion. The algorithm relies on the motion-compensated noise reduction by using landmarks (balloon markers) on 45 registered frames acquired over 3–4 s [26]. These images are transferred automatically to a workstation and corrected by averaging the images from each cine frame in relation to the two balloon markers. The software enhances stent visibility, fading out anatomical structures and background noise [25]. SB was found to have good correlation with IVUS regarding stent diameter and was found to be superior to quantitative coronary angiography (QCA) [14,17,24,27–31].

Pie Medical Imaging (Maastricht, The Netherlands) introduced the CAAS StentEnhancer® (SE), a method similar to SB with the main advantage of being completely independent of the X-ray angiographic system of the vendor and hence, runs on a side station. SE uses a maximum of 40 frames from a Digital Imaging and Communications in Medicine (DICOM) file. Its algorithm automatically detects the markers of the stent balloon or of the balloon used for post-dilation in order to compute a single image in which the visibility of a deployed stent is improved. Following background subtraction, all frames are transformed into a common reference frame. The resulting images are combined into a single image after weighted averaging. A sharpening filter is then applied. This filter works by first extracting the high-frequency components from the image. These high-frequency components are then added, using a predefined amount, to the original image. High-frequency components are extracted by first creating a blurred version of the image through performing a convolution of a Gaussian filter at a predefined scale with the original image. Subtracting the blurred version from the original yields the high-frequency components. An optimally contrasted enhanced stent image is then generated to improve the visibility using a linear scaling within a predefined width around the peak pixel value which is established from a histogram analysis. Furthermore, the SE system allows for a manual contrast adjustment of the generated images as well as a quantitative assessment of the deployed stent through manual measurements of different diameters along the stent length.

Quantitative coronary angiography (QCA) is a tool to measure coronary arteries filled with contrast based on the use of a dedicated software allowing automated measurements (that can be manually corrected) of vessel diameter, percent stenosis, and minimal lumen of stent diameters [32]. After image acquisition, a digital quantification on a selected frame can be easily performed with or without magnification.

The aims of this study was to (1) qualitatively compare image results from the SE system to the currently available SB system and (2) report the comparisons between measured

diameters of deployed stents by the SE system and the expected chart diameters upon deployment and after post-dilation as well as final QCA measurements.

2. Materials and Methods

2.1. Study Design

Between January 2016 and January 2018, patients in whom an ESI acquisition was performed after the implantation of a stent at the Centre Hospitalier Universitaire et Psychiatrique de Mons-Borinage (CHUPMB), Belgium, were retrospectively reviewed. The acquired ESI images were transferred to the SB and SE workstations (CAAS workstation software v.8.4) and reconstructed. The patients' baseline demographic and procedural characteristics were collected. The study was conducted according to the guidelines of the Declaration of Helsinki and approved by the Ethics Committee of CHUPMB and Erasme-ULB (Université Libre de Bruxelles) (protocol code P2017/462 on 16 October 2017) who waived the requirement for written consent. Two independent blinded and experienced interventional cardiologists compared and graded the stent images obtained by each technique. The images from the same sequence (SB and SE) were blindly compared side to side (on the left side, it was either a SB or SE image and on the right side the other one). The images were graded on a scale from 0 to 2 (0 = undetectable; 1 = seen unclearly; and 2 = clearly seen) for different characteristics: (1) visualization of the proximal edge of the stent; (2) visualization of the distal edge of the stent; (3) clear visualization of the struts of the stent; and (4) the presence of underexpansion and (5) calcifications. One month later, 50 sequences were randomly selected and re-analyzed a second time by one of the two observers for the intra-observer variation analysis.

A subset of images was processed using a custom-designed Matlab software (version R2017a, The MathWorks, Natick, MA, USA) that computed the signal-to-noise ratio (SNR) of SB and SE images defined as the ratio of the average signal value μ_{sig} to the standard deviation σ_{bg} of the background. As shown in Figure 1, a reference noise square of 100 by 100 pixels was manually placed in a region without interventional material (wire, previous stent, etc.) and without a bone structure such as a rib. Another rectangle was then traced around the stent, as close as possible to the struts. The same two regions were used in the SB and SE images for comparison. The standard deviation σ_{bg} of the background pixel values was calculated in the square region of interest (ROI) of noise whereas the average signal value μ_{sig} was calculated as the average of the values of the pixels in the ROI traced around the enhanced stent.

Furthermore, between January 2021 and July 2022, patients with mildly to moderately calcified de novo coronary lesions in 4 Belgian centers who were treated by stent implantation and ESI acquisition in 2 orthogonal views were prospectively included. This protocol with EudraCT code B7072020000065 was approved by the Ethics Committee Hospitalo-Facultaire Universitaire de Liège under reference 2020/87 on 13/11/2020, as well as by each local institution review board. The study was also conducted according to the guidelines of the Declaration of Helsinki and informed written consent were obtained. The patients' baseline demographic and procedural characteristics were collected. The ESI images were transferred to the SE and QCA workstations (CAAS software v.8.4) and reconstructed. Of note, one center used a Siemens X-ray system with the Clearstent ESI system, the others used a Philips system with StentBoost. SE and QCA could be measured on the DICOM files from these two manufacturers. The final QCA analysis was conducted and included maximal and minimal stent diameters as well as percent stenosis. A quantitative SE analysis of the 2 orthogonal views acquired including proximal and distal stent edge diameters as well as minimal stent diameter was conducted. Mean stent diameter as well as percent stenosis were calculated in both views and compared to the expected stent chart diameter according to the pressure of deployment of the stent and after post-dilatation when available as well as to the QCA measurements. A Bland–Altman analysis was performed to compare the SE and QCA diameters.
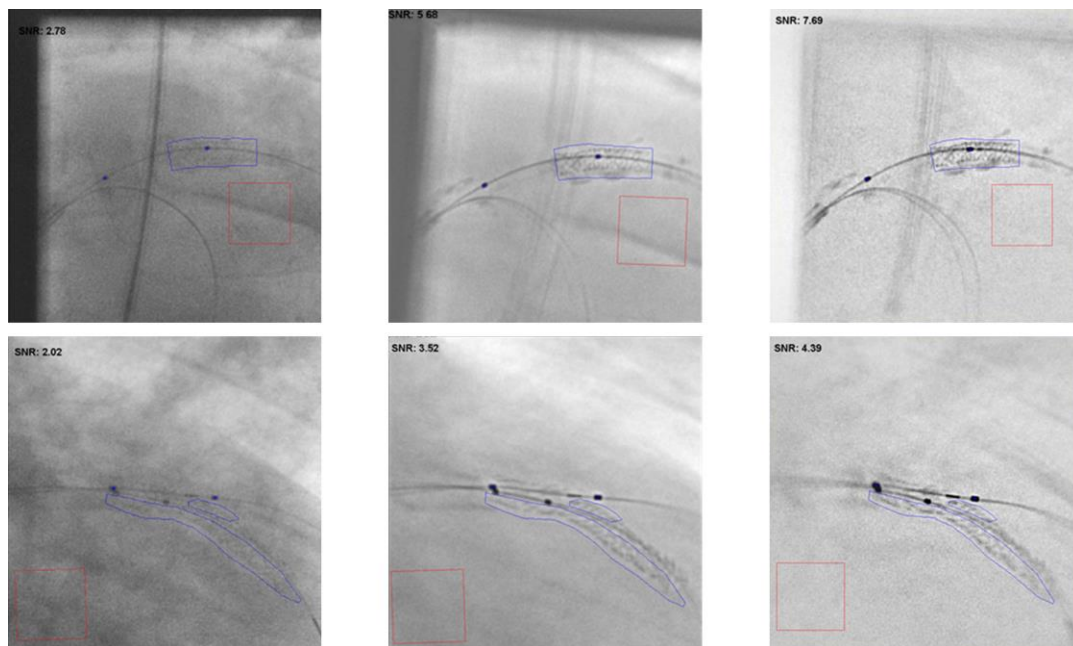
Figure 1. On the top, comparison between the original angiographic image (**left**), StentBoost (**middle**) and StentEnhancer (**right**) and the region where the noise was computed (red square) and the signal (blue region of interest around the stent). Bottom, original frame (**left**) and StentBoost (**middle**) and StentEnhancer (**right**) results where an underexpansion can be detected from the important calcifications outside of the stent. SNR in original image is 2.8, and, respectively, 5.7 and 7.7 for the SB and SE images (in area around stent).

2.2. Statistical Analysis

Categorical variables are reported as absolute values and percentages. Continuous variables are presented as means and standard deviations.

The Wilcoxon test was used to compare the two software and the two observers. After comparisons of the two methods, Kappa coefficients were calculated for repeatability and agreement between the reviewers.

The Kendall test was used to compare the two software for the presence of calcifications and stent underexpansion. Two McNemar tests were used for the evaluation of calcifications on underexpansion and post-dilatation efficacy. The SNRs of the SB and SE images were compared using a paired t-test. A p value < 0.05 was considered statistically significant. All statistical analyses was performed using SPSS software v.23 (IBM, New York, NY, USA).

3. Results

3.1. Patient and Lesion Characteristics

3.1.1. Qualitative Analysis

The qualitative analysis included 157 lesions with a total of 249 ESI sequences from 140 patients. The mean patient age was 64.7 ± 10.8 years, and 72.1% ($n = 101$) were men. Calcifications were reported on angiography in 72% ($n = 113$) of the cases. A total of 170 stents were placed, of which, 140 (82.5%) were drug-eluting stents. Post-dilatation was performed in 68% of the cases; of these, 92% used a non-compliant balloon. The lesions were deemed highly calcified for 13 lesions (8%), moderately calcified for 40 (25%), slightly calcified for 60 (38%), and free of calcifications for 44 (28%). The baseline clinical, lesion, and stent characteristics of the study population are outlined in Table 1. Out of the 157 treated lesions, 26 (17%) were ST elevation myocardial infarctions (STEMI) and 46 (29%) non-ST elevation myocardial infarctions (NSTEMI). The indication to perform PCIs for the other patients was angina pectoris or arrhythmia, with ischemia proven non-invasively or after measurement of a fractional flow reserve. There were 18 total occlusions (11%). The lesions

were localized in 34% of the cases in the right coronary artery (RCA), in 24% in the left circumflex artery (LCx), in 39% in the left anterior descending artery (LAD), and in 5% in the left main coronary artery.

Table 1. Qualitative cohort baseline clinical, lesion, and stent characteristics.

			N
Number of patients			140
Mean age (years)			64.7 ± 10.7
Male gender			101 (72.1%)
Mean body mass index (kg/m^2)			29.1 ± 5.9
Risk factors			
Hypertension			91 (65%)
Dyslipidemia			119 (85%)
Diabetes mellitus			54 (38.6%)
Current smoker			37 (26.4%)
Indication for PCI procedure			
Stable angina			45 (26.5%)
Unstable angina			
Non-ST elevation myocardial infarction			46 (27.1%)
ST elevation myocardial infarction			26 (15.3%)
Other			
Medical history			
Peripheral artery disease			38 (27.1%)
Treated coronary artery			
Number of lesions treated			157
Calcifications			113 (72%)
Left anterior descending artery			62 (39.5%)
Left circumflex artery			24 (15.3%)
Right coronary artery			53 (33.8%)
Left main coronary artery			8 (5.1%)
Other			10 (6.4%)
Stents			
Number of stents implanted			170
Coating	**Scaffold**	**Struts Thickness (µm)**	
Everolimus			
	PtCr	81	1 (0.6%)
	PtCr	74	67 (39.4%)
Sirolimus			
	CoCr	60	38 (22.4%)
	CoCr	80	29 (17.1%)
	316L	100	3 (1.8%)
	Mg	150	1 (0.6%)
Paclitaxel	PtCr	81	1 (0.6%)
TiNO	CoCr	75	5 (2.9%)
BMS			
	CoCr	80	25 (14.7%)

BMS = bare metal stent; **CoCr** = cobalt chromium; **PtCr** = platinum chromium; **TiNO** = titanium nitric oxide; **316L** = 316L stainless steel.

3.1.2. Quantitative Analysis

The quantitative analysis included 93 lesions treated in a total of 76 patients with a mean age of 69.2 ± 9.1 years, of which, 71.1% ($n = 54$) were men. The left anterior descending artery was treated in 63.4% ($n = 59$) and calcifications burden was moderate in 46.1% ($n = 35$) of cases. The baseline clinical, lesion, and stent characteristics of the study population are outlined in Table 2. A total of 98 stents were implanted with a mean diameter of 3.16 ± 0.46 mm at a mean inflation pressure of 11 ± 2 atm for which a mean

chart diameter of 3.25 ± 0.47 mm was expected. Post-dilation was performed in 82.7% (*n* = 81) of cases using a non-compliant balloon in 85.5% (*n* = 71).

Table 2. Quantitative cohort baseline clinical, lesion, and stent characteristics.

		N
Number of patients		76
Mean age (years)		69.2 ± 9.1
Male gender		54 (71.1%)
Mean body mass index (kg/m^2)		28.1 ± 4.6
Risk factors		
Hypertension		56 (73.7%)
Dyslipidemia		57 (75.0%)
Diabetes mellitus		28 (36.8%)
Current smoker		12 (15.8%)
Family history of heart disease		24 (31.6%)
Peripheral vascular disease		8 (10.5%)
Previous myocardial infarction		14 (18.4%)
Previous PTCA		26 (34.2%)
Renal impairment		2 (2.6%)
Indication for PCI procedure		
Chronic coronary syndrome		28 (36.8%)
Unstable angina		6 (7.9%)
Non-ST elevation myocardial infarction		5 (6.6%)
Silent ischemia		37 (48.7%)
Treated coronary artery		
Number of lesions treated		93
Calcifications burden		
	Mild	29 (38.2%)
	Moderate	35 (46.1%)
	Severe	12 (15.8%)
Lesion classification (AHA/ACC)		
	A	6 (6.5%)
	B1	62 (66.7%)
	B2	22 (23.7%)
	C	3 (3.3%)
Left anterior descending artery		59 (63.4%)
Left circumflex artery		8 (8.6%)
Right coronary artery		25 (26.9%)
Left main coronary artery		1 (1.1%)
Stents		
Number of stents implanted		98
Mean stent diameter (mm)		3.16 ± 0.46
Mean stent length (mm)		25 ± 9
Mean deployment pressure (atm)		11 ± 2
Expected chart diameter (mm)		3.25 ± 0.47
Post-dilation performed		81 (82.7%)
Non-compliant balloon		71 (85.5%)
Mean maximal post-dilatation balloon diameter (mm)		3.57 ± 0.54
Mean maximal balloon inflation pressure (atm)		18 ± 3

ACC/AHA = American College of Cardiology and the American Heart Association.

3.2. ESI Image Quality Evaluation

Table 3 shows the evaluation results of the two observers. The proximal and distal edge visualization grades did not differ between the two observers (1.42 ± 0.77 vs. 1.38 ± 0.62 and 1.46 ± 0.76 vs. 1.44 ± 0.61 for observer 1 and 2, respectively); however, a statistically significant difference (*p* < 0.05) was found between the mean total grade from observer 1 vs. observer 2 (4.12 ± 1.73 vs. 3.67 ± 1.49, respectively) for the evaluation of SB images

(Figure 1). A statistically significant difference ($p < 0.05$) was also found between the mean total grade from observer 1 vs. observer 2 (4.10 ± 1.86 vs. 3.76 ± 1.58, respectively) for the evaluation of SE images with no statistically significant difference noted for the proximal and distal edge visualization grades (1.46 ± 0.79 vs. 1.42 ± 0.64 and 1.43 ± 0.77 vs. 1.46 ± 0.59 for observer 1 and 2, respectively).

Table 3. Qualitative analysis of SB and SE.

	Observer 1		Observer 2		*p*-Value
	SE	**SB**	**SE**	**SB**	
Stent strut visibility	1.28 ± 0.73	1.35 ± 0.68	0.98 ± 0.69	0.96 ± 0.61	<0.001
Proximal stent edge visibility	1.46 ± 0.79	1.42 ± 0.77	1.42 ± 0.64	1.38 ± 0.62	NS
Distal stent edge visibility	1.43 ± 0.77	1.46 ± 0.76	1.46 ± 0.59	1.44 ± 0.61	NS
Total score	4.10 ± 1.86	4.12 ± 1.73	3.76 ± 1.58	3.67 ± 1.49	<0.001
Inter-observer Kappa coefficients (*n* = 249)					
	SE			**SB**	
Stent strut visibility	0.456			0.344	
Proximal edge visibility	0.434			0.498	
Distal edge visibility	0.416			0.386	
Stent underexpansion	0.394			0.480	
Calcifications	0.352			0.447	
Intra-observer Kappa coefficients (n = 50)					
Stent strut visibility	0.760			0.557	
Proximal edge visibility	0.629			0.710	
Distal edge visibility	0.647			0.783	
Stent underexpansion	0.584			0.473	
Calcifications	0.674			0.477	

NS = non-significant; **SB** = StentBoost; **SE** = StentEnhancer. Mean values of parameters graded out of 2 points and total score graded out of 6 points.

A Wilcoxon test demonstrated a statistically significant difference between the two observers ($p < 0.001$) indicating that they assessed the visualization of struts differently. This demonstrates the variability in such a qualitative assessment of any angiographic parameter.

The Kappa coefficients were calculated between the two observers (inter-observer Kappa) and between two different evaluations by the same observer (intra-observer Kappa). The evaluation system was simplified to a binary one. Inter-observer agreement between the two reviewers was observed (coefficient < 50% for the proximal stent edge with SB). The stent underexpansion and calcification coefficients showed similar results (coefficient < 48%). The intra-observer Kappa coefficients showed low reproducibility with perhaps a better reproducibility for the SB.

There was no significant difference between the two methods, SB or SE, according to the Wilcoxon test for each observer (Table 4). A final Kendall test demonstrated a significant difference between the two observers for the assessment of underexpansion and calcifications (Figure 2). While the first reviewer found a correlation of $\pm 60\%$, the second one found $\pm 90\%$ (Table 5). This called for a more quantitative assessment of underexpansion which we validated prospectively in the second part of this research project.

Table 4. Different mean values of parameters by observer.

		SE	SB	*p*-Value
Observer 1	Stent strut visibility	1.28 ± 0.73	1.35 ± 0.68	NS
	Proximal edge visibility	1.46 ± 0.79	1.42 ± 0.77	NS
	Distal edge visibility	1.43 ± 0.77	1.35 ± 0.68	NS
	Total score	4.10 ± 01.86	4.12 ± 1.73	NS
Observer 2	Stent strut visibility	0.98 ± 0.69	0.96 ± 0.61	NS
	Proximal edge visibility	1.42 ± 0.64	1.38 ± 0.62	NS
	Distal edge visibility	1.46 ± 0.59	1.44 ± 0.61	NS
	Total score	3.76 ± 1.58	3.67 ± 1.49	NS

NS = non-significant; **SB** = StentBoost; **SE** = StentEnhancer. Mean values of parameters graded out of 2 points and total score graded out of 6 points.
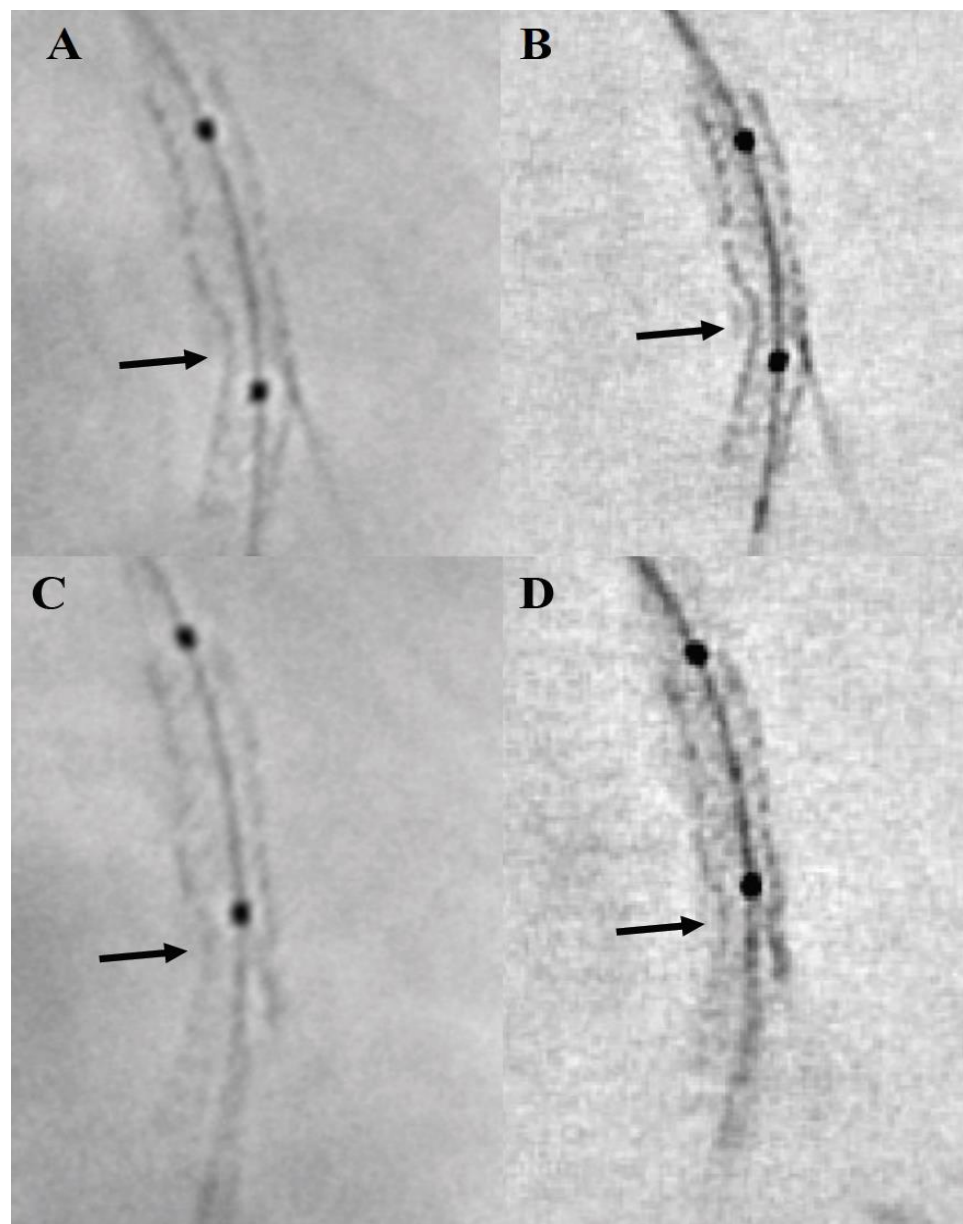

Figure 2. Underexpansion images before and after post-dilation (arrows). (**A**) StentBoost image before post-dilation; (**B**) StentEnhancer image before post-dilation; (**C**) StentBoost image after post-dilation; (**D**) StentEnhancer image after post-dilation.

Table 5. Comparison of rates of calcifications and underexpansion by SE and SB.

			SE	SB	Kendall Coefficient
Observer 1		Stent underexpansion (%)	71.5	73.9	61
		Calcifications (%)	64.0	43.8	58
Observer 2		Stent underexpansion (%)	47.0	47.0	92
		Calcifications (%)	63.9	62.7	91

3.3. Signal-to-Noise Ratio

The calculated SNR on a random part of the image and around the stent struts for a selection of 53 original frames was higher for SB and SE compared to the original frames (3.2 ± 1.0; 4.3 ± 1.5 and 2.2 ± 0.3, respectively). The SNR was statistically significantly higher for SE compared to SB ($p < 0.01$), as shown in Figure 3.
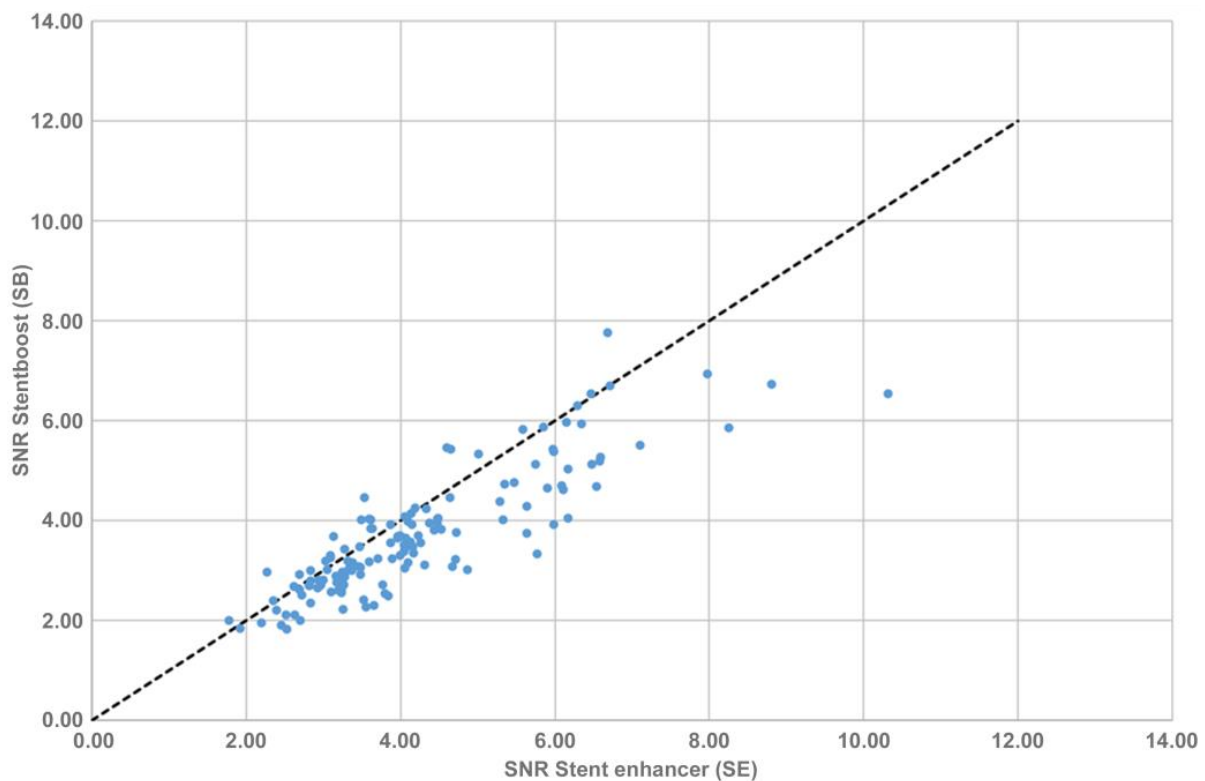
Figure 3. Linear regression between SNRs of StentBoost and StentEnhancer on 53 different frames.

3.4. Quantitative Analysis

Out of 93 lesions, reliable QCA analysis could be performed on the final PCI result in 90 lesions. Foreshortening or the overlap of branches precluded the analysis in five lesions. The mean stent diameter on QCA after stent implantation was 2.74 ± 0.53 mm and differed significantly from the predicted chart diameter ($p < 0.05$). On average, the predicted chart diameter upon stent implantation was 0.44 ± 0.44 mm larger than the mean stent diameter on QCA (95% CI; 0.34 to 0.53). This was also found upon comparison of mean stent diameter by QCA and maximal achieved post-dilation balloon diameter ($p < 0.001$). The stents diameters found by QCA tended to be 0.74 ± 0.48 mm smaller than

the maximal achieved balloon diameter upon post-dilation (95% CI; 0.62 to 0.84). The remaining stents could not be quantified due to vessel overlapping.

A quantitative SE analysis could be performed in more stents (n = 91) using both orthogonal views after deployment of the stent and following post-dilation (Figure 4). The mean stent diameter post-implantation was 2.96 ± 0.45 mm (90% of predicted chart diameter) which was statistically different from the expected chart diameter ($p < 0.001$). The expected chart diameter was on average 0.31 ± 0.30 mm larger than the SE diameter (95% CI; 0.25 to 0.38). There was no statistically significant difference between the measured mean stent diameters and the measured diameters at the maximal stent underexpansion point between the two orthogonal views upon implantation (2.95 ± 0.46 mm vs. 2.95 ± 0.49 mm and 2.39 ± 0.46 mm vs. 2.44 ± 0.47 mm, respectively; $p > 0.05$). The mean stent diameter after post-dilatation by SE was 3.13 ± 0.49 mm (84% of predicted balloon diameter) and was, on average, 0.47 ± 0.31 mm smaller than the balloon diameter (95% CI; 0.39 to 0.56). The mean maximal stent underexpansion upon deployment was 19 ± 9% and 16 ± 7% after post-dilation. There was no statistically significant difference in the measured mean stent diameters between the two orthogonal views after post-dilation (3.11 ± 0.48 mm vs. 3.18 ± 0.55 mm; $p > 0.05$); however, a statistically significant difference was noted for the measured diameter at the site of maximal stent underexpansion point between the two views after post-dilation (2.58 ± 0.52 mm vs. 2.69 ± 0.52; $p = 0.004$). The achieved mean diameter by SE after post-dilation was more in line with the expected chart diameter upon implantation with a mean difference of 0.13 ± 0.32 mm (95% CI; 0.04 to 0.21). A statistically significant diameter gain of 0.23 ± 0.23 mm was noted at the site of maximal stent underexpansion after balloon post-dilation was noted upon comparison of mean minimal stent diameters upon implantation and after post-dilation (2.41 ± 0.44 mm vs. 2.63 ± 0.49 mm, respectively; $p < 0.001$). The detailed quantitative analysis results can be found in Table 6. The mean stent diameters after stent deployment by SE were, on average, 0.41 ± 0.44 mm [95% CI; 0.06 to 0.23] larger than the mean stent diameters by QCA ($p < 0.05$) and were 0.32 ± 0.38 mm [95% CI; 0.05 to 0.22] larger after post-dilation ($p < 0.05$).

Table 6. QCA and SE measurements.

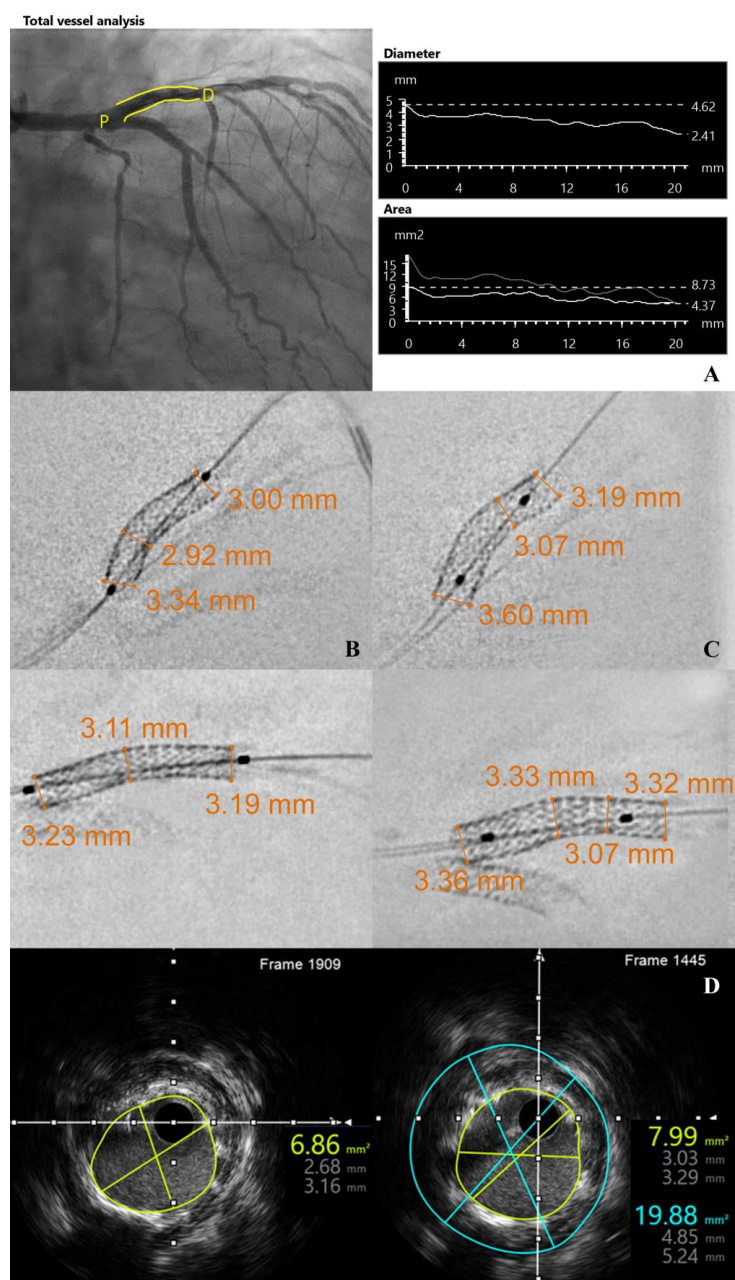| QCA Analysis	
Post-Stent Implantation	n = 14
Mean stent diameter (mm)	2.74 ± 0.53
Minimal in-stent diameter (mm)	2.26 ± 0.48
Percentage stenosis (%)	13.86 ± 9.54
Post-balloon post-dilation	n = 75
Mean stent diameter (mm)	2.84 ± 0.53
Minimal in-stent diameter (mm)	2.23 ± 0.46
Percentage stenosis (%)	14.7 ± 11.9
SE analysis	
Mean stent diameter at deployment (mm)	2.96 ± 0.47
Minimal in-stent diameter at deployment (mm)	2.41 ± 0.44
Deployment diameter to chart (%)	90 ± 9
Mean stent underexpansion at deployment (%)	19 ± 9
Mean stent diameter after post-dilation (mm)	3.13 ± 0.49
Minimal in-stent diameter after post-dilation (mm)	2.63 ± 0.49
Post-dilation diameter to balloon (%)	13 ± 2
Mean stent underexpansion after post-dilation (%)	16 ± 7

Figure 4. Quantitative analysis of an implanted proximal left anterior descending stent. Panel (**A**): quantitative coronary angiography analysis; Panel (**B**): StentEnhancer quantitative analysis post-implantation in two orthogonal views; Panel (**C**): StentEnhancer quantitative analysis after post-dilation. Stent expansion could be evaluated visually with clear stent struts and minimal calcifications. The pixels were transformed into millimeters using the calibration of the image. Note the presence of a second stent implanted in the ramus intermedius. Panel (**D**): Intravascular images at the minimal cross-sectional area in the stent after implantation (**left**) and after post-dilatation (**right**).

4. Discussion

The current study qualitatively compared the inter- and intra-observer results of different image criteria of a novel ESI software (SE) to the market-available one (SB) as well as a quantitative analysis of SE.

The results of the two ESI algorithms were compared as per each observer and finally SNRs for the two methods were calculated and compared to the SNR calculated from the angiographic image. ESI methods have been demonstrated to enhance contrast on fluoroscopic images, allowing better visualization of stent struts. This study demonstrated

that SE is not inferior to SB for the criteria evaluated but a clear inter-observer variability calls for more quantitative methods. Despite this difference, both observers had a preference towards SE images to study parameters. SE can be easily integrated into procedures, independent of the X-ray angiography machine vendor, and was found in our study to provide good stent expansion assessment as well as a better stent strut visualization. The SNR of SE images was found to be superior compared to SB. We cannot provide a definite answer why this was the case, since we are unaware of the exact methods of StentBoost. However, based on the available papers, there are methodological differences. For instance, SB does not seem to perform background subtraction as can be seen in Figure 1.

Since newer generation scaffolds tend to use thinner struts or bioresobable materials in order to reduce the risk of stent thrombosis in addition to a trend towards the use of lower X-ray power during angiographic procedures, proper stent visualization is becoming challenging [3,20–23]. The use of ESI becomes pivotal for the assessment of proper stent expansion, a major risk factor for stent thrombosis [6–10].

QCA remains an important, readily available, and easy-to-use tool during PCIs allowing for a more practical and standardized angiography-based approach. QCA is particularly useful for the evaluation of the minimal lumen diameter, the reference vessel diameter, the diameter stenosis percentage, the lesion length, the acute gain, and late loss [14]. Our data failed to show any correlation between the expected stent diameter and the QCA-derived one. This could be explained by the foreshortening drawback of QCA as well as the two-dimensional evaluation by QCA of a three-dimensional vessel.

Our data demonstrated the feasibility of an accurate, quantitative, contrast-free assessment of stent expansion by SE. Post-dilatation remains an important step towards stent optimization. Our results are in-line with the current published literature in regard to the achieved stent diameter at a given implantation pressure being at least 10% lower than the given expected chart diameter [33,34]. These results could be attributed to the fact that the figures provided on the compliance charts are derived from bench tests performed in water at 37 °C while QCA and SE are measured on stents deployed in fibrotic and calcified lesions. The diameters measured by SE remain 2-dimensional measurements of a 3-dimensional structure. A second measurement using an orthogonal view would therefore overcome this limitation. The measured mean stent diameters by SE did not differ when using the two orthogonal views indicating precise measurements between the two views. However, a difference was noted for the measurements at the site of maximal stent underexpansion after post-dilation. This could be attributed to the eccentricity of lesions as well as to the visual assessment of the minimal diameter compared to adjacent ones.

Despite an era where modern flat-detector technology allows excellent angiographic images, coronary stent visualization has become a challenge especially with the on-going reduction in stent strut thickness. Stents are often suboptimally visualized on plain angiography hence limiting optimal PCI outcomes. High temporal resolution is needed to qualify a moving structure.

Adequate stent expansion has important short- and long-term effects after PCIs in clinical practice. It is crucial, yet challenging, to detect suboptimal stent deployment on qualitative and quantitative angiography since it is associated with an increased rate of in-stent restenosis and stent thrombosis [3,20]. Current stent delivery systems are still suboptimal for stent expansion, requiring, in most cases, a post-dilation using a larger, higher pressure, non-compliant balloon to improve the in-lumen area. This is particularly true when increased calcifications are found [24,35] as we demonstrated in our 157 lesions.

Intracoronary imaging, including intravascular ultrasound and optical coherence tomography, remains more sensitive than angiography and QCA in determining stent under expansion as illustrated in Figure 4; their use was found to improve stent expansion results and long term outcome [6,20,36]. However, these techniques are limited by cost, time, and technical expertise, calling for a simpler, ready-to-use visualization method. ESI was found very useful in identifying stents under expansion, thereby improving PCI outcomes [37]. Image processing algorithm softwares based on X-ray angiography images

offer better stent visualization compared to angiography alone as validated by several previous studies [24,38]. ESI also shows no risk of complications and adds little additional time or radiation to the procedure [25,37]. Furthermore, ESI allows accurate measurements of the dimension of stents [29]. It was found useful in obese patients, long lesions, in-stent restenosis, and bifurcating lesions. Moreover, ESI was found to be superior to QCA and angiography and was highly correlated with IVUS [17,28,28,30,38].

We performed a comparison between the final diameters measured by QCA and by SE. We had 14 paired data available with no post-dilatation and 75 after final post-dilatation in the other patients. As shown in Figure 5, on average, the mean difference was -0.37 ± 0.42 mm and this bias for smaller QCA diameters was significant, with the 95% confidence interval not encompassing the 0. Using IVUS as the reference, Goto et al. also demonstrated that QCA underestimates MLDs in small vessels (<3.8 mm) and over-estimates MLDs in vessels larger than 3.8 mm [39]. A direct head-to-head comparison of IVUS and SE might confirm a better agreement between IVUS and SE than with QCA. The wide agreement window between QCA and SE of ± 0.84 mm reflects the differences in the two methodologies, with only manual measurements being currently possible with the SE images, while automated contour calculation and minimal and reference diameters are available with QCA. However, when there were overlap of side branches or other vessels, no QCA could be reliably measured in 3 out of the 93 cases. Without contrast, hence without any overlap, SE could always be measured. Of note, no reliable reconstruction can be calculated on very long stents and/or with long balloons when the markers are more than 30 mm apart. Several ESI softwares are currently available on the market but each one can only be used on the specific vendor's angiographic system. The StentEnhancer software computes enhanced fluoroscopy images using the balloon markers as references, delivering an easily integrated, high-quality image independent of the angiography instrument vendor. Although an increase in radiation was reported during ESI acquisition, no significant impact on the patient radiation dose was found [40].
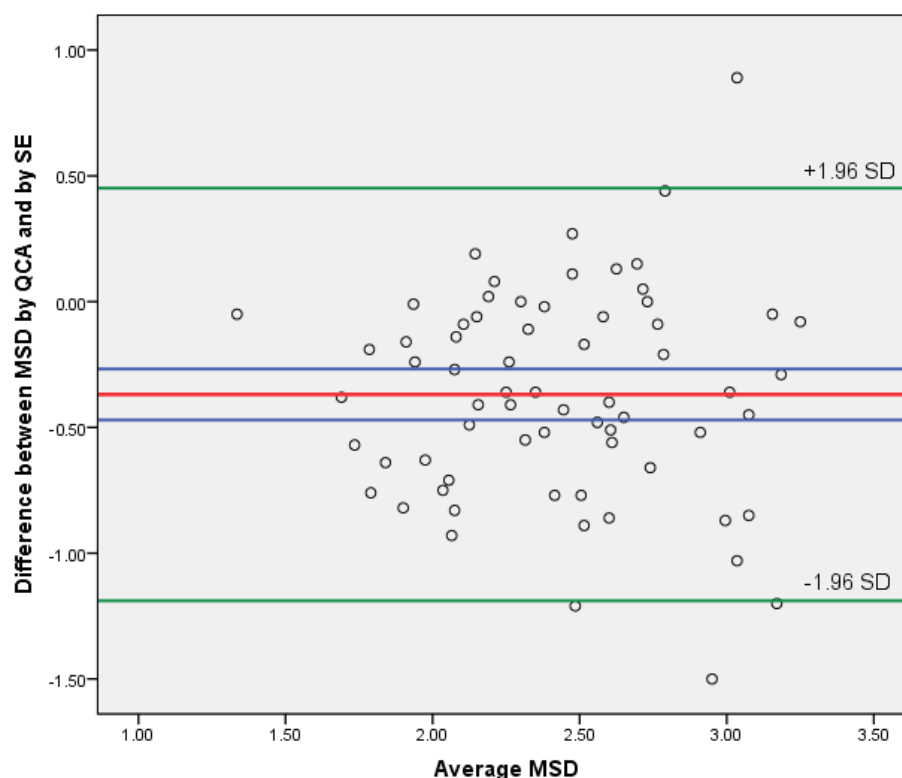

Figure 5. Bland-Altman analysis comparing QCA and SE. Red line: mean; green lines: 1.96 × SD; blue lines: 95%CI; circles: individual measurements. MSD: minimal stent diameter; SE: StentEnhancer; SD: standard deviation; QCA: quantitative coronary angiography.

5. Conclusions

StentEnhancer is a novel ESI modality that provides enhanced stent visualization and allows quantitative assessment of stent underexpansion. It is a simple, cost-effective, and minimally invasive method. We demonstrate that it is not inferior qualitatively to the validated StentBoost software on the market providing good stent visualization. The StentEnhancer workstation also allowed for a quantitative analysis of images to obtain stent expansion measurement as well as stent underexpansion quantitative assessment. A comparative study between StentEnhancer images and IVUS is needed in order to further validate the StentEnhancer measurements.

Author Contributions: Conceptualization, C.G., C.C., K.H. and S.C.; methodology, C.G.; software, C.G. and C.C.; validation, S.C., J.D., P.K. and C.U.; formal analysis, C.G. and C.C.; writing—original draft preparation, C.G.; writing—review and editing, S.C.; supervision, S.C. All authors have read and agreed to the published version of the manuscript.

Funding: This research received no external funding.

Data Availability Statement: Research data are available upon request.

Conflicts of Interest: The authors declare no conflict of interest.

References

1. Neumann, F.J.; Sechtem, U.; Banning, A.P.; Bonaros, N.; Bueno, H.; Bugiardini, R.; Chieffo, A.; Crea, F.; Czerny, M.; Delgado, V.; et al. 2019 ESC Guidelines for the Diagnosis and Management of Chronic Coronary Syndromes. *Eur. Heart J.* **2020**, *41*, 407–477. [CrossRef]
2. Kawaguchi, R.; Angiolillo, D.J.; Futamatsu, H.; Suzuki, N.; Bass, T.A.; Costa, M.A. Stent Thrombosis in the Era of Drug Eluting Stents. *Minerva Cardioangiol.* **2007**, *55*, 199–211. [PubMed]
3. Gopalakrishnan, M.; Lotfi, A. Stent Thrombosis. *Semin. Thromb. Hemost.* **2018**, *44*, 046–051. [CrossRef] [PubMed]
4. Choi, S.Y.; Maehara, A.; Cristea, E.; Witzenbichler, B.; Guagliumi, G.; Brodie, B.; Kellett, M.A.; Dressler, O.; Lansky, A.J.; Parise, H.; et al. Usefulness of Minimum Stent Cross Sectional Area as a Predictor of Angiographic Restenosis after Primary Percutaneous Coronary Intervention in Acute Myocardial Infarction (from the HORIZONS-AMI Trial IVUS Substudy). *Am. J. Cardiol.* **2012**, *109*, 455–460. [CrossRef]
5. Serruys, P.W.; Kay, I.P.; Disco, C.; Deshpande, N.V.; De Feyter, P.J. Periprocedural Quantitative Coronary Angiography after Palmaz-Schatz Stent Implantation Predicts the Restenosis Rate at Six Months: Results of a Meta-Analysis of the Belgian Netherlands Stent Study (BENESTENT) I, BENESTENT II Pilot, BENESTENT II and MUSIC. *J. Am. Coll. Cardiol.* **1999**, *34*, 1067–1074. [CrossRef]
6. Fujii, K.; Carlier, S.G.; Mintz, G.S.; Yang, Y.M.; Moussa, I.; Weisz, G.; Dangas, G.; Mehran, R.; Lansky, A.J.; Kreps, E.M.; et al. Stent Underexpansion and Residual Reference Segment Stenosis Are Related to Stent Thrombosis after Sirolimus-Eluting Stent Implantation: An Intravascular Ultrasound Study. *J. Am. Coll. Cardiol.* **2005**, *45*, 995–998. [CrossRef] [PubMed]
7. Okabe, T.; Mintz, G.S.; Buch, A.N.; Roy, P.; Hong, Y.J.; Smith, K.A.; Torguson, R.; Gevorkian, N.; Xue, Z.; Satler, L.F.; et al. Intravascular Ultrasound Parameters Associated with Stent Thrombosis After Drug-Eluting Stent Deployment. *Am. J. Cardiol.* **2007**, *100*, 615–620. [CrossRef] [PubMed]
8. Moussa, I.; Di Mario, C.; Reimers, B.; Akiyama, T.; Tobis, J.; Colombo, A. Subacute Stent Thrombosis in the Era of Intravascular Ultrasound-Guided Coronary Stenting without Anticoagulant: Frequency, Predictors and Clinical Outcome. *J. Am. Coll. Cardiol.* **1997**, *29*, 6–12. [CrossRef] [PubMed]
9. Choi, S.Y.; Witzenbichler, B.; Maehara, A.; Lansky, A.J.; Guagliumi, G.; Brodie, B.; Kellett, M.A.; Dressler, O.; Parise, H.; Mehran, R.; et al. Intravascular Ultrasound Findings of Early Stent Thrombosis after Primary Percutaneous Intervention in Acute Myocardial Infarction: A Harmonizing Outcomes with Revascularization and Stents in Acute Myocardial Infarction (HORIZONS-AMI) Substudy. *Circ. Cardiovasc. Interv.* **2011**, *4*, 239–247. [CrossRef]
10. Cheneau, E.; Leborgne, L.; Mintz, G.S.; Kotani, J.; Pichard, A.D.; Satler, L.F.; Canos, D.; Castagna, M.; Weissman, N.J.; Waksman, R. Predictors of Subacute Stent Thrombosis: Results of a Systematic Intravascular Ultrasound Study. *Circulation* **2003**, *108*, 43–47. [CrossRef]
11. Nerlekar, N.; Cheshire, C.J.; Verma, K.P.; Ihdayhid, A.R.; McCormick, L.M.; Cameron, J.D.; Bennett, M.R.; Malaiapan, Y.; Meredith, I.T.; Brown, A.J. Intravascular Ultrasound Guidance Improves Clinical Outcomes during Implantation of Both First- and Second generation Drug-Eluting Stents: A Meta-Analysis. *EuroIntervention* **2017**, *12*, 1632–1642. [CrossRef]
12. Buccheri, S.; Franchina, G.; Romano, S.; Puglisi, S.; Venuti, G.; D'Arrigo, P.; Francaviglia, B.; Scalia, M.; Condorelli, A.; Barbanti, M.; et al. Clinical Outcomes Following Intravascular Imaging-Guided Versus Coronary Angiography–Guided Percutaneous Coronary Intervention with Stent Implantation: A Systematic Review and Bayesian Network Meta-Analysis of 31 Studies and 17,882 Patients. *JACC Cardiovasc. Interv.* **2017**, *10*, 2488–2498. [CrossRef]

13. Maehara, A.; Matsumura, M.; Ali, Z.A.; Mintz, G.S.; Stone, G.W. IVUS-Guided Versus OCT-Guided Coronary Stent Implantation: A Critical Appraisal. *JACC Cardiovasc. Imaging* **2017**, *10*, 1487–1503. [CrossRef] [PubMed]
14. Ghafari, C.; Carlier, S. Stent Visualization Methods to Guide Percutaneous Coronary Interventions and Assess Long-Term Patency. *World J. Cardiol.* **2021**, *13*, 416–437. [CrossRef] [PubMed]
15. Truesdell, A.G.; Alasnag, M.A.; Kaul, P.; Rab, S.T.; Riley, R.F.; Young, M.N.; Batchelor, W.B.; Maehara, A.; Welt, F.G.; Kirtane, A.J. Intravascular Imaging During Percutaneous Coronary Intervention: JACC State-of-the-Art Review. *J. Am. Coll. Cardiol.* **2023**, *81*, 590–605. [CrossRef] [PubMed]
16. Lee, J.M.; Choi, K.H.; Song, Y.B.; Lee, J.-Y.; Lee, S.-J.; Lee, S.Y.; Kim, S.M.; Yun, K.H.; Cho, J.Y.; Kim, C.J.; et al. Intravascular Imaging–Guided or Angiography-Guided Complex PCI. *N. Engl. J. Med.* **2023**, *388*, 1668–1679. [CrossRef]
17. Tanaka, N.; Pijls, N.H.J.; Koolen, J.J.; Botman, K.J.; Michels, H.R.; Brueren, B.R.G.; Peels, K.; Shindo, N.; Yamashita, J.; Yamashina, A. Assessment of Optimum Stent Deployment by Stent Boost Imaging: Comparison with Intravascular Ultrasound. *Heart Vessels* **2013**, *28*, 1–6. [CrossRef]
18. Kastrati, A.; Mehilli, J.; Dirschinger, J.; Dotzer, F.; Schühlen, H.; Neumann, F.J.; Fleckenstein, M.; Pfafferott, C.; Seyfarth, M.; Schömig, A.; et al. Intracoronary Stenting and Angiographic Results: Strut Thickness Effect on Restenosis (Isar Stereo) Trial. *Circulation* **2001**, *103*, 2816–2821. [CrossRef]
19. Pache, J.; Kastrati, A.; Mehilli, J.; Schühlen, H.; Dotzer, F.; Hausleiter, J.; Fleckenstein, M.; Neuman, F.J.; Sattelberger, U.; Schmitt, C.; et al. Intracoronary Stenting and Angiographic Results: Strut Thickness Effect on Restenosis Outcome (ISAR-STEREO-2) Trial. *J. Am. Coll. Cardiol.* **2003**, *41*, 1283–1288. [CrossRef]
20. Mutha, V.; Asrar Ul Haq, M.; Sharma, N.; Den Hartog, W.F.; Van Gaal, W.J. Usefulness of Enhanced Stent Visualization Imaging Technique in Simple and Complex PCI Cases. *J. Invasive Cardiol.* **2014**, *26*, 552–557.
21. Doi, H.; Maehara, A.; Mintz, G.S.; Weissman, N.J.; Yu, A.; Wang, H.; Mandinov, L.; Popma, J.J.; Ellis, S.G.; Grube, E.; et al. Impact of In-Stent Minimal Lumen Area at 9 Months Poststent Implantation on 3-Year Target Lesion Revascularization–Free Survival. *Circ. Cardiovasc. Interv.* **2008**, *1*, 111–118. [CrossRef]
22. Ohlmann, P.; Mintz, G.S.; Kim, S.W.; Pichard, A.D.; Satler, L.F.; Kent, K.M.; Suddath, W.O.; Waksman, R.; Weissman, N.J. Intravascular Ultrasound Findings in Patients with Restenosis of Sirolimus- and Paclitaxel-Eluting Stents. *Int. J. Cardiol.* **2008**, *125*, 11–15. [CrossRef]
23. Iantorno, M.; Lipinski, M.J.; Garcia-Garcia, H.M.; Forrestal, B.J.; Rogers, T.; Gajanana, D.; Buchanan, K.D.; Torguson, R.; Weintraub, W.S.; Waksman, R. Meta-Analysis of the Impact of Strut Thickness on Outcomes in Patients with Drug-Eluting Stents in a Coronary Artery. *Am. J. Cardiol.* **2018**, *122*, 1652–1660. [CrossRef] [PubMed]
24. Sanidas, E.A.; Maehara, A.; Barkama, R.; Mintz, G.S.; Singh, V.; Hidalgo, A.; Hakim, D.; Leon, M.B.; Moses, J.W.; Weisz, G. Enhanced Stent Imaging Improves the Diagnosis of Stent Underexpansion and Optimizes Stent Deployment. *Catheter. Cardiovasc. Interv.* **2013**, *81*, 438–445. [CrossRef] [PubMed]
25. Rogers, R.K.; Michaels, A.D. Enhanced X-Ray Visualization of Coronary Stents: Clinical Aspects. *Cardiol. Clin.* **2009**, *27*, 467–475. [CrossRef]
26. Zaid, A.O.; Hadded, I.; Belhaj, W.; Bouallegue, A.; Abdessalem, S.; Mechmeche, R. Improved Localization of Coronary Stents Based on Image Enhancement. *Int. J. Biomed. Sci.* **2008**, *4*, 212–216. [PubMed]
27. Laimoud, M.; Nassar, Y.; Omar, W.; Abdelbarry, A.; Elghawaby, H. Stent Boost Enhancement Compared to Intravascular Ultrasound in the Evaluation of Stent Expansion in Elective Percutaneous Coronary Interventions. *Egypt. Heart J.* **2018**, *70*, 21–26. [CrossRef]
28. Zhang, J.; Duan, Y.Y.; Jin, Z.G.; Wei, Y.J.; Yang, S.L.; Luo, J.P.; Ma, D.X.; Jing, L.M.; Liu, H.L. Stent Boost Subtract Imaging for the Assessment of Optimal Stent Deployment in Coronary Ostial Lesion Intervention: Comparison with Intravascular Ultrasound. *Int. Heart J.* **2015**, *56*, 37–42. [CrossRef]
29. Davies, A.G.; Conway, D.; Reid, S.; Cowen, A.R.; Sivananthan, M. Assessment of Coronary Stent Deployment Using Computer Enhanced X-Ray Images-Validation against Intravascular Ultrasound and Best Practice Recommendations. *Catheter. Cardiovasc. Interv.* **2013**, *81*, 419–427. [CrossRef]
30. Blicq, E.; Georges, J.L.; Elbeainy, E.; Gibault-Genty, G.; Benjemaa, K.; Jerbi, B.; Livarek, B. Detection of Stent Underdeployment by Stentboost Imaging. *J. Interv. Cardiol.* **2013**, *26*, 444–453. [CrossRef]
31. Omran, O.M.; Sherif, M.H.; Saied, E.S.; El-Ashmawy, M.M.; El-guindy, A.D.; El-den, S.M.S. Evaluation of Coronary Stent Expansion during Percutaneous Coronary Interventions Using Stent Boost Visualization in Comparison with Intravascular Ultrasound. *J. Adv. Med. Med. Res.* **2022**, *34*, 205–215. [CrossRef]
32. Garrone, P.; Biondi-Zoccai, G.; Salvetti, I.; Sina, N.; Sheiban, I.; Stella, P.R.; Agostoni, P. Quantitative Coronary Angiography in the Current Era: Principles and Applications. *J. Interv. Cardiol.* **2009**, *22*, 527–536. [CrossRef] [PubMed]
33. Lozano, I.; López-Palop, R.; Pinar, E.; Pérez-Lorente, F.; Picó, F.; Valdés, M. Comparison between Theoretical and Actual Intracoronary Stent Dimensions in Non-Complex Lesions. *Rev. Española Cardiol.* **2006**, *59*, 624–627. [CrossRef]
34. De Ribamar Costa, J.; Mintz, G.S.; Carlier, S.G.; Costa, R.A.; Fujii, K.; Sano, K.; Kimura, M.; Lui, J.; Weisz, G.; Moussa, I.; et al. Intravascular Ultrasonic Assessment of Stent Diameters Derived from Manufacturer's Compliance Charts. *Am. J. Cardiol.* **2005**, *96*, 74–78. [CrossRef] [PubMed]

35. Blasini, R.; Neumann, F.J.; Schmitt, C.; Bökenkamp, J.; Schömig, A. Comparison of Angiography and Intravascular Ultrasound for the Assessment of Lumen Size after Coronary Stent Placement: Impact of Dilation Pressures. *Cathet. Cardiovasc. Diagn.* **1997**, *42*, 113–119. [CrossRef]

36. Hong, M.-K. Intravascular Ultrasound Predictors of Angiographic Restenosis after Sirolimus-Eluting Stent Implantation. *Eur. Heart J.* **2006**, *27*, 1305–1310. [CrossRef] [PubMed]

37. Silva, J.D.; Carrillo, X.; Salvatella, N.; Fernandez-Nofrerias, E.; Rodriguez-Leor, O.; Mauri, J.; Bayes-Genis, A. The Utility of Stent Enhancement to Guide Percutaneous Coronary Intervention for Bifurcation Lesions. *EuroIntervention* **2013**, *9*, 968–974. [CrossRef] [PubMed]

38. Cura, F.; Albertal, M.; Candiello, A.; Nau, G.; Bonvini, V.; Tricherri, H.; Padilla, L.T.; Belardi, J.A. StentBoost Visualization for the Evaluation of Coronary Stent Expansion during Percutaneous Coronary Interventions. *Cardiol. Ther.* **2013**, *2*, 171–180. [CrossRef]

39. Goto, K.; Mintz, G.S.; Litherland, C.; Lansky, A.J.; Weisz, G.; McPherson, J.A.; De Bruyne, B.; Serruys, P.W.; Stone, G.W.; Maehara, A. Lumen Measurements from Quantitative Coronary Angiography and IVUS: A PROSPECT Substudy. *JACC Cardiovasc. Imaging* **2016**, *9*, 1011–1013. [CrossRef] [PubMed]

40. Jin, Z.; Yang, S.; Jing, L.; Liu, H. Impact of StentBoost Subtract Imaging on Patient Radiation Exposure during Percutaneous Coronary Intervention. *Int. J. Cardiovasc. Imaging* **2013**, *29*, 1207–1213. [CrossRef]